Uncertainty quantification in the Gamow Shell Model

J. Wylie[1,2] and D. Lay[1,2]

[1] *FRIB/NSCL Laboratory, Michigan State University, East Lansing, Michigan 48824, USA*
[2] *Department of Physics and Astronomy, Michigan State University, East Lansing, Michigan 48824, USA*

(Dated: July 18, 2023)

Nuclei near the drip lines are excellent examples of Open Quantum Systems. The development and implementation of new theoretical models to describe these systems have produced many interesting insights into underlying nuclear phenomena. This work outlines the general strategy for performing a full Bayesian uncertainty quantification for one such model - the Gamow Shell Model.

I. INTRODUCTION

Nuclear structure problems can be roughly classified into two groups: Closed Quantum Systems (CQS) and Open Quantum Systems (OQS). CQS-type problems treat an object as a completely isolated system from which no external factors can influence its properties. OQS are featured across physics - from macroscopic, molecular, systems to mesoscopic, nuclear, systems - and have shared phenomena in the form of resonances and scattering states.

In the nuclear context, the primary focus is to study weakly-bound states or resonances which are inherent to OQS. Resonances are particularly interesting as they are a result of coupling between bound and scattering states in nuclei and are typically found in the "Correlation dominated" region of Figure 1. For a more physical definition of a resonance, we could say that it is associated with a specific energy which produces a substantial increase in the cross section of a nucleus (the probability of an interaction occurring). In other words, a resonance is a local band of an energy region where a projectile can alter the structure of a nucleus without ever being bound or knocking another particle from the target. Essentially, a resonance is a feature in a nucleus where the lifetime of exotic states is extended beyond what one might typically assume to be short lived in the CQS picture.

One framework which has been implemented to explore nuclear resonances and, more generally, continuum coupling is the Gamow Shell Model (GSM). Fundamentally, it is similar to the traditional nuclear shell model (SM), which is built on the assumption that nucleons (protons or neutrons) prefer to structure themselves in a particular order to form nuclear states. In the case of the ground state of a nucleus this ordering is the configuration which minimizes the total energy of the nucleus. Although this concept was proposed very early (1932) and has been refined over the decades (and GSM is one such refinement of the SM), there has been little effort taken in performing a full Bayesian study to quantify the uncertainties in these models. This paper will propose a general strategy one might take when performing uncertainty quantification (UQ) for GSM - and follow it through for a tractable case for light nuclei - but many of the concepts and workflow could be generalized to other models.

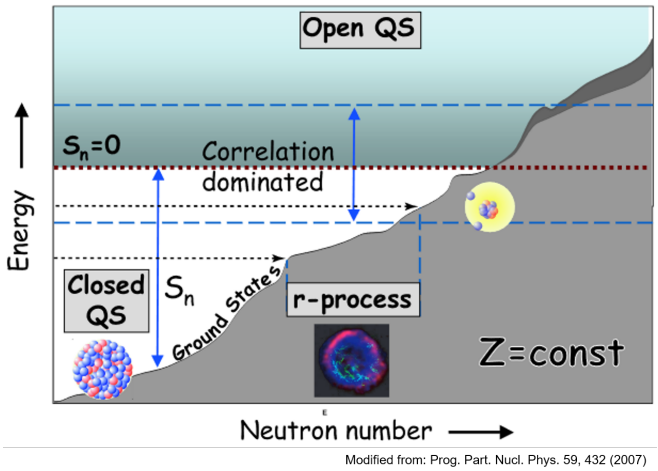

FIG. 1. Illustration of openness in (increasingly neutron-rich) nuclear systems and the emergence of exotic phenomena at energies closer to threshold ($S_n = 0$) due to increases in the ground state energy.

II. GSM FRAMEWORK

GSM has many concepts which are familiar to those aware of the regular SM. We start by assuming a well-bound core (at least relative to our nucleus of interest) and add a number of nucleons on top of that, called valence nucleons. These valence nucleons will interact with the core and each other just like in the SM. GSM then includes effects of the continuum via the Berggren basis [1]. We can control the level of openness of the system by limiting the number of these valence nucleons that are allowed to interact with the continuum. This is sometimes necessary due to large sizes of our calculations; in general, Bayesian UQ can be prohibitively expensive due to the time and resources required for each calculation.

Before we get too far into the details of UQ, we will provide a brief overview of the important components to GSM which will be of interest. A full description can be found in Ref. [1] for anyone interested. Fundamentally, we are solving the Schrödinger equation

$$H\left|\Psi\right\rangle = \tilde{E}\left|\Psi\right\rangle, \quad \text{with} \quad \tilde{E} = E - \frac{i\Gamma}{2} \tag{1}$$

for a many-body system whose wave functions $|\Psi\rangle$ are

represented by Slater Determinants, built from single particle states, and the complex energy eigenstate $\tilde{E}$ which contains a real energy (E) and the decay width of the system (Γ). The GSM Hamiltonian can be expressed as

$$H = \sum_{i}^{N_{\rm val}} \left[\frac{\vec{p}_i^2}{2\mu_i} + U_c(i) \right] + \sum_{i=1,j>i}^{N_{\rm val}} \left[V_{i,j} + \frac{\vec{p}_i \vec{p}_j}{M_c} \right] \quad (2)$$

with $N_{\rm val}$ denoting the number of valence nucleons and μ_i, M_c being the reduced mass of the nucleon and core respectively. U_c is the core-nucleon potential which contains Woods-Saxon (WS), spin-orbit, and Coulomb terms

$$U_c(r) = V_0 f(r) - 4V_{\ell s} \frac{1}{r} \frac{df(r)}{dr} \vec{\ell} \cdot \vec{s} + U_{\rm Coulomb}(r)$$
$$\text{where} \quad f(r) = \frac{-1}{1 + \exp\left[r - R_0\right]/a}. \quad (3)$$

$V_{i,j}$ is the valence nucleon-nucleon interaction. This Hamiltonian is written in terms of cluster-orbital shell model coordinates with respect to the core's center of mass. This interaction term can be decomposed as

$$V = V_c + V_{\rm LS} + V_T + V_{\rm Coulomb}, \quad (4)$$

or the central, spin-orbit, tensor, and Coulomb terms. The first three are based on the Furutani-Horiuchi-Tamagaki (FHT) force, and are written based on spin-isospin projectors (Π_{ST})

$$\begin{aligned} V_c(r) &= V_c^{11} f_c^{11}(r) \Pi_{11} + V_c^{10} f_c^{10}(r) \Pi_{10} \\ &\quad + V_c^{00} f_c^{00}(r) \Pi_{00} + V_c^{01} f_c^{01}(r) \Pi_{01} \\ V_{LS} &= \left(\vec{L} \cdot \vec{S} \right) V_{LS}^{11} f_{LS}^{11}(r) \Pi_{11} \\ V_T(r) &= S_{ij} \left[V_T 11 f_t^{11}(r) \Pi_{11} + V_T^{10} f_t^{10}(r) \Pi_{10} \right] \end{aligned} \quad (5)$$

where $\vec{L}$ is the relative orbital angular momentum, $\vec{S} = (\vec{\sigma_i} + \vec{\sigma_j})/2$, and $S_{ij} = 3(\vec{\sigma}_i \cdot \hat{r})(\vec{\sigma}_j \cdot \hat{r}) - \vec{\sigma}_i \cdot \vec{\sigma}_j$. The distance between nucleons i and j is represented by r_{ij} and $\hat{r} = \vec{r}_{ij}/r_{ij}$. It should be noted that there are a number of nucleon-nucleon interactions one could pick for V and this is just one possible case.

III. OBSERVABLES AND PRIORS

As we saw in Sec. II, there are a number of different parameters we can adjust in the Hamiltonian. The primary parameters which tend to be adjusted are the core-nucleon terms V_0 and $V_{\ell s}$ (for protons and neutrons) and the nucleon-nucleon FHT terms ($V_{\rm type}^{ij}$) in Eq. 5 (7 total). For the sake of completeness, we can also include the WS radius r_0 and diffuseness d for proton and neutron potentials. In total this adds up to 16 model parameters which would be contained in θ.

An initial set of these parameters, obtained via χ^2 minimization for light nuclei in [2], is presented in Table I. These will serve as the starting point for our initial calculations. Note that only 4 of the nucleon-nucleon interaction parameters were nonzero. In other words, we will use these parameters for our priors $P(\theta)$ where $\theta = (d^n, d^p, r_0^n, r_0^p, V_0^p, V_{\ell s}^p, V_0^n, V_{\ell s}^n, V_c^{01}, V_c^{10}, V_c^{00}, V_T^{10})$ with 12 parameters.

TABLE I. Parameters optimized in Ref. [2] and their errors. When applicable, for the core-nucleon interactions only, we present the different parameters for protons and neutrons; otherwise, the parameters are shared for all nucleon types. Those parameters not listed are set to 0.

Parameter	Neutrons	Protons
V_0 (MeV)	39.5 (2)	42.1 (4)
$V_{\ell s}$ (MeV fm^2)	10.7 (2)	11.1 (5)
V_c^{01} (MeV)	-9.425 (70)	
V_c^{10} (MeV)	-8.309 (90)	
V_c^{00} (MeV)	-8.895 (1130)	
V_T^{10} (MeV)	-22.418 (970)	

In order to provide experimental insight into our calculations, we will choose to study the nuclei (and a select number of their states) listed in Table II whose experimental energies and decay widths are known. We only picked $A = 5, 6$ due to the rapid increase in model space size with increasing number of particles in the continuum - while 1 or 2 valence nucleons is quite manageable for a few hundred calculations, 3 or more is not. Another advantage to using only these A values is that they should largely be described by configurations only being in $\ell = 1$ as the $0s_{1/2}$ state is occupied by the core and the next highest angular momenta would be in the sd shells. This then simplifies the number of parameters we need in θ as each WS and spin-orbit potential are ℓ-dependent.

Since GSM uses a complex energy formalism (Eq. 1) we will take the real and imaginary parts of the GSM complex energies to compare to the experimental energies and decay widths. This separation is justified as the two experimental observables are subject to different experimental error values. More importantly, sometimes decay widths are not reproduced even when the energy is well constrained to an experimental value in GSM. A more in-depth debate about which observables to include can certainly be had, but for the purposes of this simple guide, is not necessary. This also prevents us from having complex values in our likelihood function - keeping the formalism simple. This gives us 12 energies and 12 decay widths (24 observables total). Ideally, we might pick another quantity which is available across most nuclei to serve as another check.

TABLE II. Experimental data for each nucleus. Energy is relative to α core i.e. $E = (4\times{}^4\text{He(BE/A)}) - (A\times{}^A_Z\text{X(BE/A)})$ and are taken from [3].

Nucleus	State	E^{exp} (MeV)	Γ^{exp} (keV)
^{5}He	$3/2^-$	0.735 (20)	0.60 (2)
^{5}Li	$3/2^-$	1.97 (5)	1.23×10^3
^{6}Be	0^+	1.372 (9)	92 (6)
^{6}Be	2^+	3.042 (50)	1160 (60)
^{6}He	0^+	-0.975 (9)	0 ($\sim$ 0)
^{6}He	2^+	0.822 (5)	113 (20)
^{6}Li	1^+_0	-3.698 (3)	0 ($\sim$ 0)
^{6}Li	3^+_0	-1.512 (2)	24 (2)
^{6}Li	0^+_0	-0.1351 (1)	8.2×10^{-3} (2)
^{6}Li	2^+_0	0.614 (22)	1.3×10^3 (1)
^{6}Li	2^+_1	1.677 (15)	541 (20)
^{6}Li	1^+_1	1.952 (50)	1.3×10^3 (2)

IV. CHOOSING OUR LIKELIHOOD FUNCTION

Now that we have data to compare to and have identified our priors we can try to identify the form of our likelihood function. If we consider applying our model using the prior parameters identified in Table I, we can get an initial estimate of how our model might deviate from experiment. Assuming our model (y_i^{model}) is fixed and the deviation from experiment is

$$y_i^{\text{exp}} = y_i^{\text{model}} + \delta_i + \epsilon_i \tag{6}$$

where the experimental error for each measurement is ϵ_i, then the difference between experimental and model results when including said error is

$$\delta_i = y_i^{\text{exp}} - y_i^{\text{model}} - \epsilon_i. \tag{7}$$

Now, we can think of δ_i as a random variable because - assuming we find a reasonable form - it can be reproduced in such a way that any generated pseudo-data would be indistinguishable from the true data set. This concept is illustrated in Figure 2.

Since we're treating δ as a random variable, we can attempt to assign it to a distribution. Considering the difference between the model results (calculated with our parameters in Table I) and experiment we see in Figure 3 that the difference between the decay widths is centered about zero and could be characterized as a Gaussian. Unfortunately, it is harder to identify a reasonable distribution to assign the energies; however, as this paper is a preliminary discussion of the methods used, we can assign this as a Gaussian for simplicity at this point. The characterization of the priors can certainly be revisited and perhaps improved with more insight, so we emphasize that *the choice is always up to what the user thinks is the best representation.*

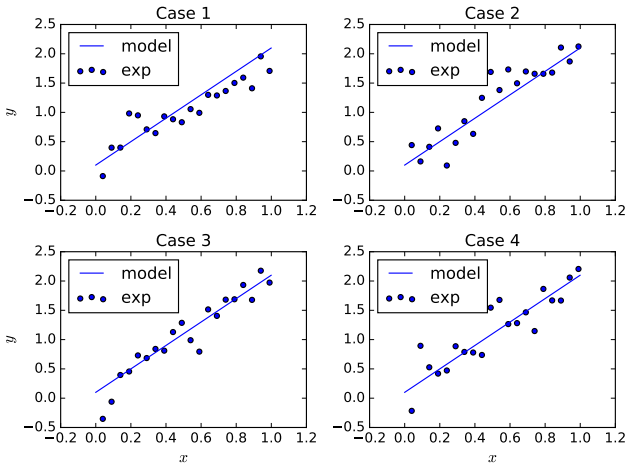

FIG. 2. Simple depiction of δ contribution to a system which is described as $y_i^{\text{exp}} = y_i^{\text{model}}(x) + \delta_i + \epsilon_i$ where $y_i^{\text{model}}(x) = \theta_1 x + \theta_2$. We see that if δ is treated as randomly distributed, we can generate data which is indistinguishable from the original dataset (set 1).

From this point, we have identified that both $\epsilon_i \sim \mathcal{N}\left(0, (\sigma_i^{\text{exp}})^2\right)$ and $\delta_i \sim \mathcal{N}\left(0, (\sigma_i^{\text{model}})^2\right)$. Our likelihood function is even simpler to construct if we assume each measurement is independent of one another. Then,

$$P(\boldsymbol{Y}|\theta) = P(y_1|\theta)P(y_2|\theta)...P(y_N|\theta) \tag{8}$$

$$= \frac{1}{\left(2\pi\sigma^2_{\text{total}}\right)^{N/2}} \prod_{i=1}^{N} \exp\left(-\frac{(y_i^{\text{model}} - y_i^{\text{exp}})^2}{2\sigma^2_{\text{total}}}\right)$$

$$= \frac{1}{\left(2\pi\sigma^2_{\text{total}}\right)^{N/2}} \exp\left(-\sum_{i=1}^{N} \frac{(y_i^{\text{model}} - y_i^{\text{exp}})^2}{2\sigma^2_{\text{total}}}\right) \tag{9}$$

where $\left(\sigma_i^{\text{total}}\right)^2 = \left(\sigma_i^{\text{exp}}\right)^2 + \left(\sigma_i^{\text{model}}\right)^2$. For this case, the form follows because the sum of two Gaussians is another Gaussian; for generic likelihood models (for independent data), see e.g. [4] for a list of common forms.

V. CALCULATING THE POSTERIORS

To determine our posteriors, we simply need to follow Bayes theorem

$$P(\theta|\boldsymbol{Y}) \propto P(\boldsymbol{Y}|\theta)P(\theta). \tag{10}$$

and thus can begin our UQ process. The normalization term $P(\boldsymbol{Y})$ term will be accounted for when performing the Monte Carlo operations described below. Randomly sampling the parameter space θ from the likelihood lets us generate a list of θ values for M sample sets, $\theta_1, \theta_2, ...\theta_M$. When pulling a set of parameters from our likelihood, we will tend to randomly sample the regions centered around our priors. This is shown conceptually for an arbitrary set of parameters V_0^p and V_c^{00} in Figure

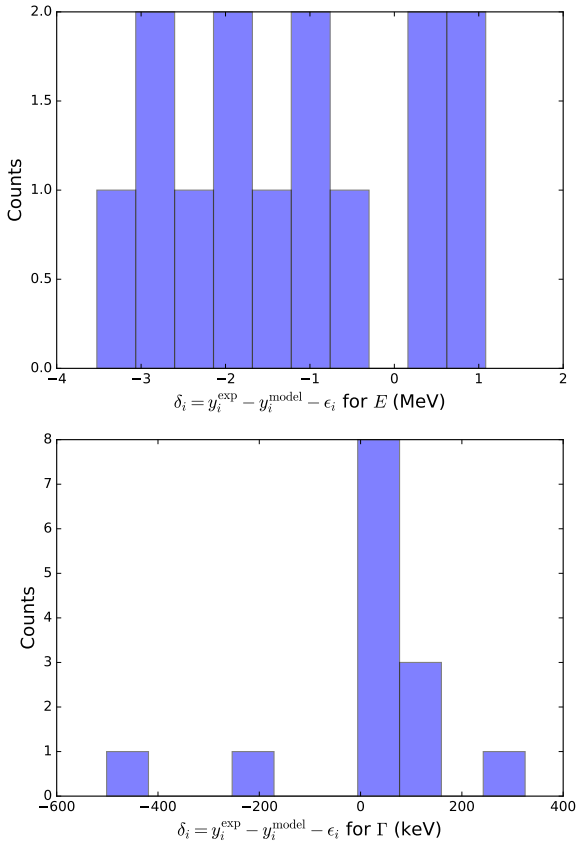

FIG. 3. Histograms of values of δ_i which were obtained with Eq. 7 using the GSM results from a few already calculated nuclei (^{6}Be$(0^+, 2^+)$, ^{6}Li$(1^+, 3^+)$, ^{6}He$(0^+, 2^+)$, ^{7}B$(3/2^-)$, ^{7}Be$(3/2^-, 1/2^-)$, ^{7}Li$(3/2^-, 1/2^-)$, and ^{7}He$(3/2^-)$) and experimental data. Since we only have 14 experimental data points for each observable (28 total), we do not have enough points to generate a good Gaussian shape.

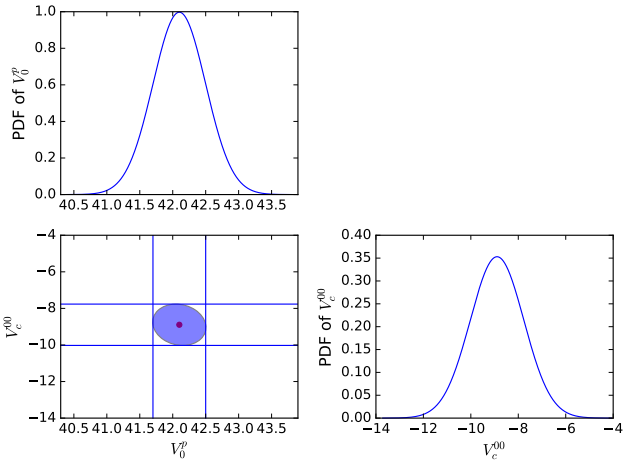

FIG. 4. Simplified depiction of sampling V_0^p and V_c^{00}. The shaded region is centered about the prior values and the shaded area represents 1σ. Their PDFs are presented as well. Note this are for illustrative purposes and not based on actual data.

4 where we will have a Monte Carlo algorithm to sample the shaded region.

Based on other Bayesian studies of nuclear models [5], we choose to use the Metropolis-Hastings algorithm for our Markov Chain Monte Carlo (MCMC) parameter sampling. This algorithm includes a random walk which has rejection criteria to effectively sample much of the shaded region in Figure 4 and traverse slightly outside it. The minimum required number of samples appears to be on the order of 10^5 samples per parameter [5], but more would improve the fidelity.

Unfortunately, even in some of the simplest cases (like the one we are currently considering) this is a significant bottleneck in UQ as each GSM calculation for some of the simplest nuclei will take on the order of 30 seconds on a personal computer. To speed up calculations, we can transition to large clusters like the High Performance Computing Center at Michigan State University, however this will still be insufficient for more complex nuclei like ^{8}C which can take 12 hours per calculation. Those familiar with these types of scaling problems will recognize that this is the perfect opportunity for the development of emulators - as was done in Ref. [5]. In this case, a proper treatment should introduce an emulator error term η which (like δ) represents the difference between the true model and the emulated version, although we do not do that here.

After using the Metropolis-Hastings algorithm to traverse our parameter space, we then input each parameter set (our $\theta_1, \theta_2, ...\theta_N$) into our model to compare their distributions to experiment (like was done in Figure 6 in Ref. [5]). This then provides uncertainty values to our model predictions for each observable.

VI. APPLICATION OF SURMISE

For our simple GSM UQ approach, we used the Surmise package [6] which provides many convenient tools which can be used for many general UQ applications. As discussed above, even calculations which take a few seconds or less on a cluster are not very feasible when dealing with sampling volumes on the order of 10^5, especially since such calculations cannot be parallelized due to the random walk nature of Metropolis-Hastings requiring information from previous iterations. In order to get around this bottleneck, we chose to use Surmise's built-in emulation packages. For this work, we use a Gaussian process, as included in Surmise; in the future, we can always use more advanced emulation techniques and substitute our custom emulators into Surmise.

To use an emulator, we still need some high-fidelity

data points at various random parameter values. This of course can be parallelized as each randomly picked set of θ's is independent of each other. Since this project was more oriented to pedagogical descriptions, we only performed 200 sets of GSM calulations for all of our states - i.e. we obtained 200 different θ sets and calculated all our states in Table II for each θ. This information was then passed into Surmise's emulator along with the experimental data and errors.

Following the construction of our emulator, we simply input it into the Bayesian calibration function of Surmise to perform our MCMC sampling. This process then allowed us to produce our results as summarized by the corner plot in Figure 5.

As we see in this figure, our results overlap very well with those calculated previously. This is rather unsurprising due to a few reasons, the first of which is the nature of the parameter set. Since we have results which were minimized, the parameters themselves should be relatively uncorrelated which they appear to be. The second is that these are already minimized with Gaussian distributions and so any valid random walks would be largely centered about their minima.

VII. CONCLUSIONS

The description of nuclei near the drip lines requires models which treat bound states, resonant states, and scattering states on equal footing, yet little work has been done to fully quantify their model uncertainties. In such exotic regions, where experimental errors are higher and the underlying physics is not as well understood, assigning uncertainties to our theoretical predictions is essential.

We have illustrated how one might approach full Bayesian UQ in GSM, but more investigation and improvements are certainly needed in every aspect. Starting from the construction of the likelihood where the decay widths seem to generally follow a normal distribution, more information to identify the distribution of δ for the energies is required.

Additionally, while a simple Gaussian process emulator might be sufficient, it is likely that more sophisticated emulators could provide better representation of GSM and its uncertainties. After all, performing this UQ process for nuclei $A \geq 6$ may require the implementation of emulators to avoid run-time bottlenecks.

This will be especially useful when considering exotic nuclei like ^{8}C or ^{9}He and ^{9}N which have few experimental measurements, and theoretical predictions with large or nonexistent error bars. Bayesian techniques will help provide better theoretical information crucial for understanding exotic phenomena with reasonable uncertainties.

[1] Nicolas Michel and Marek Płoszajczak, *Gamow Shell Model: The Unified Theory of Nuclear Structure and Reactions*, Vol. 983 (Springer, Cham, Switzerland, 2021).

[2] X Mao, J. Rotureau, W. Nazarewicz, N. Michel, R. M. Id Betan, and Y. Jaganathen, "PHYSICAL REVIEW C 102 , 024309 (2020) Gamow-shell-model description of Li isotopes and their mirror partners," Physical Review C **102**, 24309 (2020).

[3] "Evaluated and Compiled Nuclear Structure Data (ENSDF)," .

[4] Wikipedia (2023).

[5] Pablo Giuliani, Kyle Godbey, Edgard Bonilla, Frederi Viens, and Jorge Piekarewicz, "Bayes goes fast: Uncertainty quantification for a covariant energy density functional emulated by the reduced basis method," Frontiers in Physics **10** (2023), 10.3389.

[6] Matthew Plumlee, Özge Sürer, and Stefan M. Wild, *Surmise Users Manual*, Tech. Rep. Version 0.1.0 (NAISE, 2021).

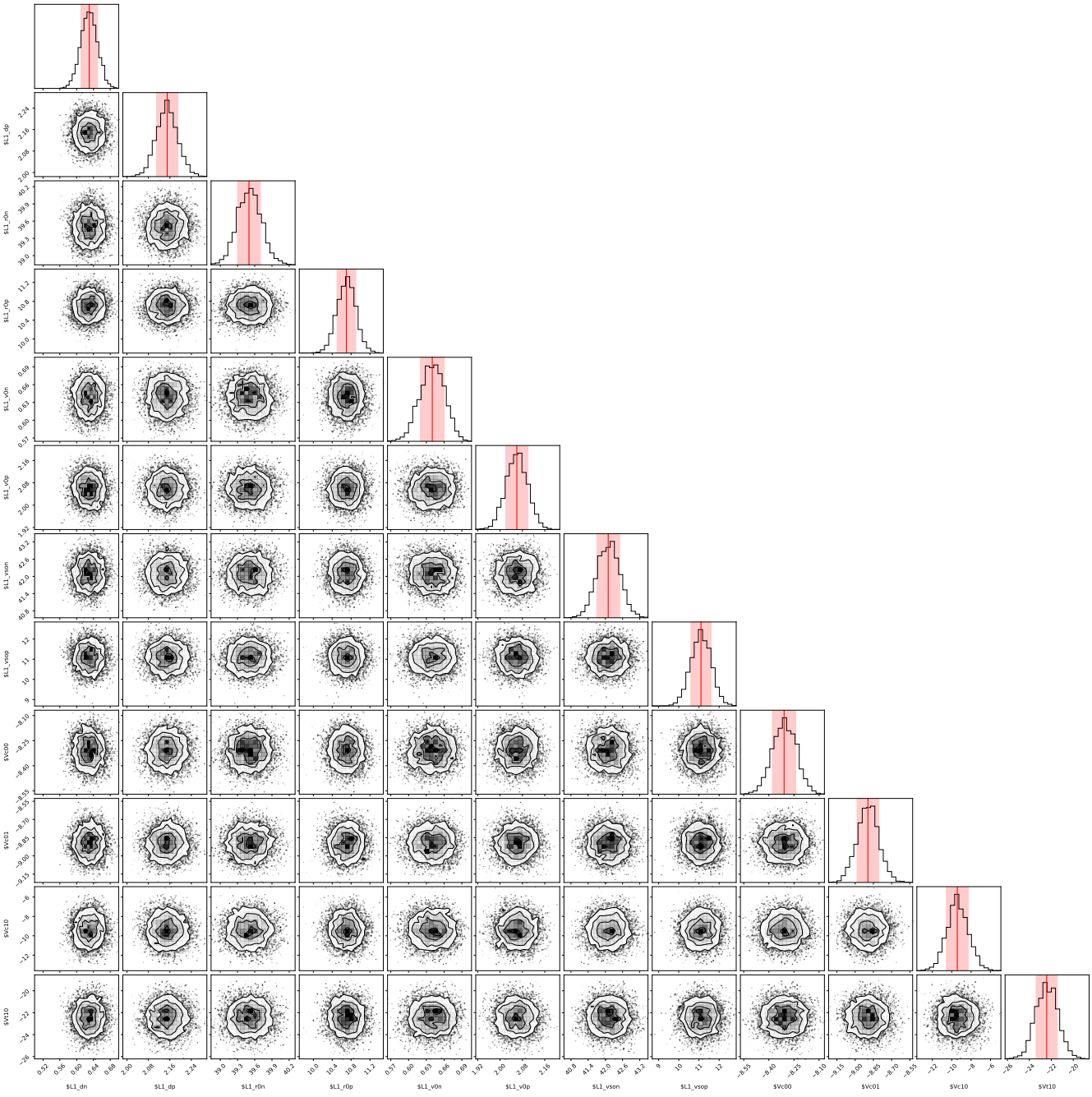

FIG. 5. Results from Bayesian calibration using Metropolis-Hastings of Surmise-emulated GSM. The red line represents the χ^2-minimized results, and the red band is a $\pm 1\sigma$ error bar, from Ref. [2].